UNIVERSITAT POLITÈCNICA DE CATALUNYA
BARCELONATECH

MASTER THESIS

A Swarm of Femtosatellites for Thermospheric Density Determination

Carlos Lledó Ardila

SUPERVISED BY

Jordi L. Gutiérrez

Universitat Politècnica de Catalunya
Master in Aerospace Science & Technology
July 2015

A Swarm of Femtosatellites for Thermospheric Density Determination

BY

Carlos Lledó Ardila

DIPLOMA THESIS FOR DEGREE

Master in Aerospace Science and Technology

AT

Universitat Politècnica de Catalunya

SUPERVISED BY:

Jordi L. Gutiérrez

Department of Applied Physics

ABSTRACT

The Lower thermosphere (between 80 and 350 km) is quite badly known due to the scarcity of satellites in this region. Nevertheless, it is an important region in several respects. Firstly, because its density determines when a falling satellite will reenter the dense layers of the atmosphere, thus affecting at reentry predictions. Secondly, it is highly relevant to understand physical processes in the atmosphere, and to study the Earth-Sun relation.

Miniaturization of electronic devices has been driven in recent years by consumer applications like smartphones and computers. However, these electronic devices can also be employed to design small but rather capable satellites with total masses below 100 grams, thus in the range of femtosatellites. Given the limited capabilities of femtosatellites in terms of power, computational capability, attitude determination and control, to cite just a few, it is important to identify the advantages of femtosatellites as compared with their larger relatives. As far as we can see, the main advantages are in cost (including launch cost) and on the possibility of launching swarms of dozens, hundreds or even thousands of femtosatellites. In any case, it is obvious that femtosatellites cannot (and should not) compete with larger satellites devoted to, for example, meteorology, communications or astronomy, at least in their standard ways of operation.

To fix the terminology, a swarm is defined as a cluster of satellites that has no control over their relative position (thus has no formation-flight nor constellation control capabilities) and are distributed over a wide area, even surrounding the whole Earth, to accomplish some mission goals. Then, a large number of femtosatellites of spherical shape would provide an instantaneous determination of atmospheric parameters simultaneously in a large number of points. These femtosatellites would include three micro-g accelerometers (to calculate the acceleration in the three axes), a microprocessor with low power consumption, a GPS, a flash memory, voltage regulators and a transmitter plus a primary battery (with a high energetic density) to feed all the systems. All these electronics, and the rest needed to perform the bus of the satellite, would be embedded in a sphere of aerogel to resist the aerodynamic heating, and the effects of atomic oxygen.

Due to their spherical shape, the ballistic coefficient for these femtosatellites is independent of the attitude. As it is reasonable, the lower the ballistic coefficient the larger the deceleration due to drag; this makes for a better measure of the acceleration, but greatly reduces the lifetime in orbit. A compromise would be to have around 1 week of orbital lifetime, and accelerations of some micro-g’s.

The main objectives of this project would be: an analysis of the current knowledge about the lower thermosphere; discussing the general trends of the mission as a whole, and describing some further difficulties or problems associated with them; making a preliminary design of the femtosatellite based on commercial–off–the–shelf (COTS) technology; and describing some possible future developments.

Dedication

The publication of this work has been possible thanks to many people who have been helping and supporting me, both morally or making important contributions during the preparation of the project.

First of all, I would like to acknowledge the support that both my parents and my big brother have given me.

Furthermore, I want to thank my thesis director Jordi Gutiérrez Cabello to dedicate a big part of his time in the development of this work despite having a lot of work.

And finally, I would like to acknowledge the unconditional support of my friends and colleagues.

Table of Contents

List of Figures

List of tables

INTRODUCTION

A couple of decades or so ago, the expression NewSpace started to find its way into the aerospace world. The idea that it tried to convey was that usual business were done by gigantic companies (dinosaurs) that failed to recognize the importance of using new technologies, as well as new philosophies, for new satellites.

Out of this new paradigm, miniaturization, which had become essential for mass consumer electronic devices, entered the realm of space. A new paradigm of very small satellites opened the entry to space to several actors (like universities, small research centers, even amateur groups and individuals), but the space community pooh-pooed the missions that could be undertaken with this approach.

Even currently, mainstream satellites use space qualified components, which are expensive, and not state-of-the-art; but they are extremely robust. For a satellite that must fulfill a complex mission, with a cost measured in tens of millions of euros, and whose launch has costed more or less a similar amount of money, the use of extremely robust components makes a lot of sense: missions must endure the harsh space environment for years with no repairing service at hand.

Trying to compete with standard satellites in the classical kinds of missions plainly does not make any sense. Small satellites (nano, pico, or femtosallites) are almost inevitably quite limited in their capabilities. So, it is very difficult to find scientific or commercial justification for a mission to observe the Earth in standard ways using a small satellite.

Nevertheless, there are missions that cannot be pursued with normal satellites but are within our reach if using small satellites, and one of the best examples are the missions needing a multitude of satellites (hereafter, a swarm).

One of these missions is the subject of this Master Thesis: the design of a swarm of femtosatellites able to determine the atmospheric density in the lower thermosphere over the whole Earth. Obviously, this is not a mission for standard satellites. The reasons are many, and go to the essence of the mission. First of all, to have success in the main scientific goal a huge number of satellites is required (hundreds, or even thousands); the cost of producing such a fleet of mainstream satellites is beyond any logic. Secondly, the life in orbit of the swarm will be very short, as atmospheric friction will deorbit the satellites in a matter of a few weeks. Thus, not only the cost of the swarm of standard satellites would be truly astronomical, but also the money would be lost in a very short time.

This document is organized as follows. In chapter 1 we offer a short introduction to the thermosphere, and to the potential applications and science of the mission under study. Chapter two gives a review of the current research on femtosatellites, with a description of the possible missions envisioned by the different teams. Chapter three is the most important one, as it gives the preliminary design of the femtosatellite. Chapter four makes a short analysis of the mission. Finally, in chapter five we draw our conclusions and describe future work.

Chapter 1

The Landscape of Femtosatellites

1.1 The uses of femtosatellites

A femtosatellite is a satellite with a total mass between 10 grams and 100 grams. Until a decade ago, the concept of femtosatellite was scarcely accepted, as the extreme limitation in mass made the system feasible, but with no achievable mission.

In the last years, nevertheless, the development of MEMS (Micro Electro Mechanics Systems) sensors has opened the possibility to develop missions than can be accomplished by femtosatellites. The best examples are given in the next section. It seems clear that femtosatellites are not usable for any kind of application, but there are some niches in which they almost are the sole option.

Femtosatellites will probably be an interesting research tool for specific applications, like distributed systems comprising a large number of nodes, or even sporting emergent phenomena. But even if this is not the case, they will serve as a test bench for new technologies, helping to climb the TRL (Technology Readiness Level) ladder in a much faster and simpler way than the current one. Given the simplicity and low cost of femtosatellites, the risk of testing a new technology will be easily affordable; and by sending a large number of this technology demonstrators, even reasonable statistics of the behaviour of the experiment will be relatively easy to obtain.

1.2 Current research

We will now give a short overview of current femtosatellite projects, describing the concept of femtosatellite and its potential advantages over conventional satellites. In addition, we also are going to see the (short) flight history of femtosatellites, as well as some current designs and tests that have been done by several institutions.

Miniaturization of electronic devices has been driven in recent years by consumer applications like smartphones and computers. However, these electronic devices can also be employed to design small but capable satellites, such as femtosatellites. Given the limited capabilities of femtosatellites in terms of power, computational capability, attitude determination and control, citing just a few, it is important to identify the advantages of femtosatellites as compared with their larger relatives.

As far as we can see, the main advantages are in cost (including launch cost) and in the possibility of launching swarms of dozens, hundreds or even thousands of femtosatellites. It is important to mention that it is possible to incorporate a full constellation of femtosatellites in a single CubeSat, and thus enabling distributed and

simultaneous measurements. Furthermore, the fact that femtosatellites may have high area/mass ratios allows new propulsion options, such as electrodynamic propulsion or solar sailing (suitable for ChipSats with few microns of thickness).

In any case, it is obvious that femtosatellites cannot (and should not) compete with larger satellites devoted to, for example, meteorology, communications or astronomy, at least in their standard ways of operation. The use of femtosatellites, then, implies new ways of conducting the mission, or missions that currently could not be conducted by standard satellites.

Regarding the flight history of the femtosatellites, we are going to describe four of the most relevant launched femtosatellites up to now, which are the *West Ford Needles*, the *Orbital Debris Radar Calibration Spheres-2* (ODERACS-2), *RyeFemSat* from Ryerson University, and Cornell's *Sprites*.

West Ford Needles are considered the first femtosatellites that have ever been launched [1]. The West Ford Needles was a project carried out by the Massachusetts Institute of Technology in 1963 to create an artificial ionosphere in order to improve military X-band communications of the United States during the Cold War. Then, a ring of 480 million copper dipole antennas with a mass of 48 µg each one was put in medium Earth orbit between 3.500 and 3.800 km high at 96 and 87 degree inclinations in order to improve the global radio communications. Although the project was a complete success, enabling radio transmissions, this technology was finally sidelined due to the development of modern communication satellites and the complains of several scientists, who claimed that these needles contributed considerably to the generation of space debris or orbital pollution. In the following picture, we can see some examples of these needles. Its low mass, on the other hand, disqualifies them as *bona fide* femtosatellites.

Figure 1.1 Some West Ford Program needles

A major setback of the West Ford experiment was the stability of the needle clouds. Due to its very small mass and moderate ratio area to mass, the needles were

subjected to the effects of radiation pressure and would re-enter in approximately three years. In 2013, nevertheless, around 46 clumps of needles (that failed to correctly deploy) were still in Earth orbit [2], illustrating the debris risk posed by retired femtosatellites in high orbits. Curiously enough, the large area to mass ratio and the low mass of the needles enabled them to reach the ground unaltered; so, we can expect to find, approximately, one of these needles per square kilometre in the Earth's surface (much more difficult than the paradigmatic needle in the haystack).

The second relevant example is also a passive femtosatellite experiment, the Orbital Debris Radar Calibration Spheres which, despite its name, also carried three tiny dipoles to avoid the polarization problems posed by spheres. It was a project carried out by NASA in 1995 in order to provide small low earth orbiting (LEO) calibration targets for the ground-based radar in Haystack (Massachusetts, USA), as well as to optical systems used for orbital debris measurements. The main objective was to calibrate the Haystack Long Range Imaging Radar (LRIR), and for this task, small radius, metallic spheres were ideal to bounce back the radar signal from Haystack. The observation strategy was to keep the radar completely still, and observe the debris that happened to cross its field of view. These measurements and resulting data processing were completely successful [3]. It is important to mention that in this flight experiment were deployed three spheres (with a mass between 0.5 and 5 kg) together with three dipoles (with a mass between 0.5 and 1.5 g), which are considered the three femtosatellites of this mission, from the Space Shuttle Discovery STS-63. Figure 1.2 shows the insignia of this mission.

Figure 1.2 Mission patch for ODERAC

Because of its small mass to area ratio, the dipoles reentered in the atmosphere after just 17 days in orbit, while the spheres, much more massive, lasted over a year.

The short history of femtosatellites ends, till the moment, with Cornell's *Sprites* or ChipSats, a project carried out by researchers of Cornell University since 2011. Its first phase consisted on the design of three ChipSats (named Sprites) of 3.8 cm^2 and around 10 g of mass each one, which were mounted on the exterior of the ISS in

order to see how they endured the extreme conditions in space. According to the researchers, they are small and light enough to behave like space dust, in such a way that they could travel by means of solar radiation pressure into deep space without fuel supply. The size of these femtosatellites is a limiting factor to be considered, and the Cornell team plans to determine how small they can be while still maintaining communication with Earth. The main idea is to develop a technology that can be sent into deep space in swarms, with each individual chip sending back its own information [4]. It is important to mention that before *Sprites*, all the femtosatellites were passive. In the following picture, it is shown an example of these Cornell *Sprites*.

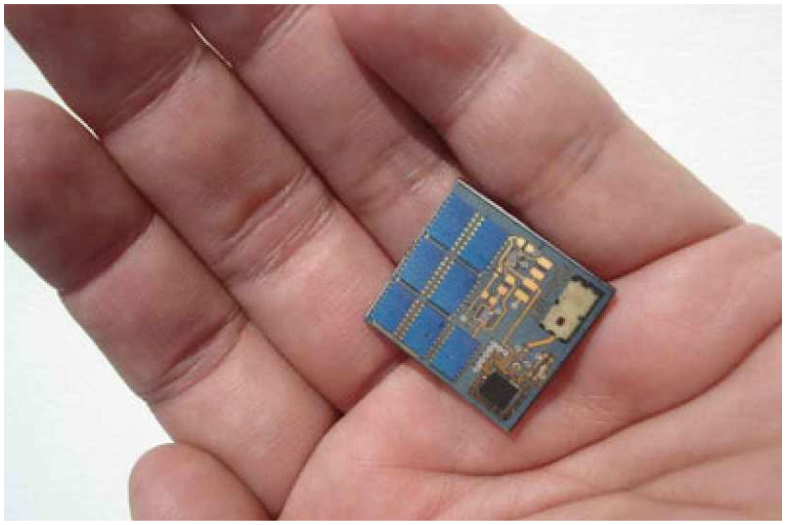

Figure 1.3 One of Cornell's Sprite femtosatellites mounted on the ISS (image courtesy Cornell University)

The three *Sprites* that were installed in the exposition experiment on-board the ISS were returned to Earth in 2014. Two of them were still properly working, while the third one was damaged (apparently, a capacitor had failed). Thus, the experiment was considered a success.

Also in 2014, a mission called *Kicksat* –also from Cornell– was launched carrying about 100 *Sprites*. *Kicksat* was a 3U Cubesat whose task was deploying the *Sprites* once in orbit. As the height was just 335 km, the swarm of femtosatellites would not pose a significant debris risk to any satellite as they would swiftly reenter. However, an anomalous reset of the master clock of *Kicksat* (probably due to the impact of a high energy particle) caused a delay on the deployment, and the satellite reentered before launching the *sprites*. The mission was thus considered a failure.

Each *Sprite* had an area 3.5×3.5 cm^2, and a mass of just under 5 g. The power subsystem consisted in two Spectrolab TASC (Triangular Advanced Solar Cells) solar cells, and a voltage regulation system to feed the several onboard MEMS devices. Under ideal conditions, these solar cells would deliver 60 mA at 2.2 V. The satellites do not have any kind of power storage, and so would be inactive during the

eclipse phase. The total power consumption was about 77 mW, less than the actual one produced by the solar cells.

It also had a Texas Instruments CC430 system-on-chip (SoC) with the MSP430 microcontroller, and a CC1101 radio mounted on the same chip, both with flight inheritance from Cubesat missions. Finally, the system had a Honeywell HMC5883L 3-axis MEMS accelerometer, and an Invensense ITG-3200 MEMS magnetometer.

The antenna was made of a memory allow, nitinol, that would deploy once in space by solar heating. It was a half dipole, and was isotropic; this was necessary as *Sprites* do not have any kind of attitude control. The transmissions are scheduled at 437.240 MHz, and the ground stations will be based on software-defined radio (SDR) to keep the cost as low as possible.

As can be seen, in its current state of development, *Sprites* are just the bus of a satellite, with no sensors or payload.

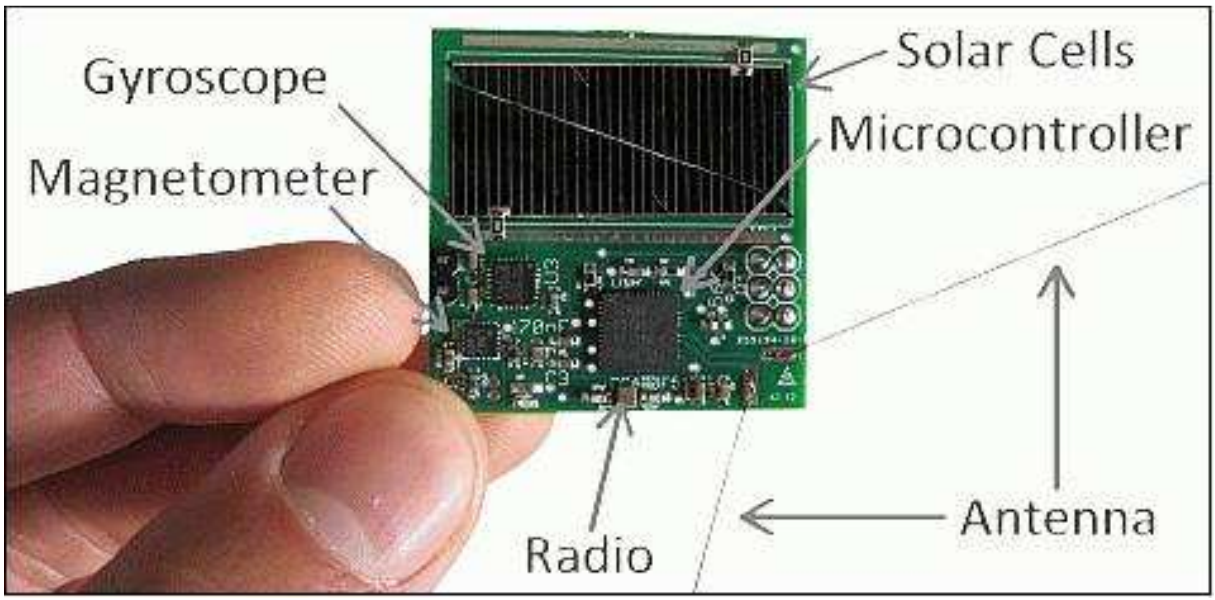

Figure 1.4 Sprite flown on Kicksat (image courtesy Cornell University)

In February 2015, NASA announced that *Kicksat*-2, a re-flight mission, had been scheduled for a launch as a part of the ELANA program. At the moment of writing this document (July 2015) the launch had no proposed date.

In 2002, a group of researchers for the Aerospace Corporation described a way to laser-etch some components (particularly, structural ones) for a 100 grams satellite out of glass/ceramic materials (Huang et al., 2002). The goal of this femtosatellite, named *Co-Orbital Satellite Assistant* (*COSA*), was to assist a larger satellite for housekeeping and operations. To make the femtosatellite capable of free-flying, Janson et al. (2004) envisioned a cold-gas thruster with 5 grams of reaction mass. *COSA* was designed to be cheap and mass-producible.

Femtosatellites are designed in two form factors: flat satellites and three dimensional ones. The flat satellites are easier to construct, as PCB technology is well spread, but sport serious problems of thermal control due to the large ratio surface to mass. The temperature excursions of these satellites are usually too large to ensure its correct operation; in particular, in full solar illumination, the temperature overcomes the maximum operational temperature, while in eclipse it descends even under the survival temperature

Regarding the current designs and tests that are being carried out, we are going to highlight two of the most relevant designs of femtosatellites, which are the *RyeFemSat* and the femtosatellite prototype made by researchers of the University of Surrey. In both cases the design of that of a PCBSat (satellite-on-a-printed circuit board). The only femtosatellite, to the best of our knowledge, with a three dimensional form factor is our *AtmoSwarm*.

RyeFemSat consists of the design and test of a femtosatellite bus prototype with a PCBSat form factor; it is being made by researchers of Ryerson University (Canada). As usual, they employ commercial-off-the-shelf (COTS) components in order to reduce both the total cost and the development time of the satellite. This femtosatellite has a total mass less than 75 g with an astounding payload capacity of 25 g (to be selected by final users).

Thanks to its mass, the satellite is able to have a 3-axis attitude determination and control based in magnetic actuators (magnetorquers). The torquers are produced on the rim of the PCB board (leaving a conducting path around the PCB), and are able to generate a tiny moment of 5 nN·m.

Command and Data Handling is produced by the Texas Instruments CC2510. The radio is embedded in the CC2510, and uses a flat patch antenna, which provides a gain of 5 dBm. The transmitted power is 27 dBm (0.5 W), and the data rate is 2400 bit/s; this provides an ample margin for high quality communications (a minimum of 40 dB in the worst case). The communications are performed in S band, at 2.450 GHz.

Power is provided by a set of solar cells, able to produce a maximum power of just over 1.5 W, and an average power of 0.347 W. This is enough for standard operations of the satellite. There are also Li-polymer batteries to feed the satellite during eclipse, and on periods of above-the-average power requirements, as is the case when the transmitter is active (and thus draining 2.1 W of power).

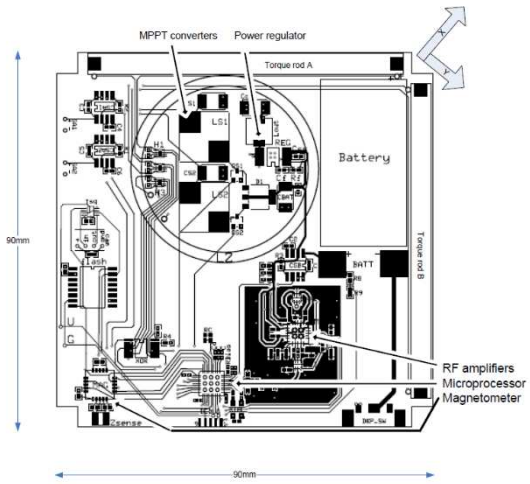

Figure 1.5 *RyeFemSat* blueprints (courtesy Ryerson University)

The primary (load carrying) structure is the PCB fiberglass, which must be subjected to vibrations tests to prove its resistance. The size of the PCB is such that it would fit inside a CubeSat, thus allowing multiple launches. In this latter case, the primary structure would be that of the CubeSat, and the PCB would be relieved of such task.

It is important to mention that the *RyeFemSat* can have applications for Earth observation missions or be used as inspector satellite for LEO (Low Earth Orbit) [5]. In figure 1.5, we can see an illustration of this PCBSat.

Finally, the PCBSat designed by the University of Surrey consists of a prototype with a unit cost less than 300$, and whose main objective is determining what capabilities can be incorporated in a femtosatellite of 100 g with the use of commercial-off-the-shelf (COTS) components. The design team further restricted their choices not only to COTS, but to the most common and accessible COTS components, and whenever possible additionally limited the choices to surface mount devices. It is then a purely technological demonstration of cheap, mass producible femtosatellites [6]. In the following picture, the front and back side of the PCBSat are shown.

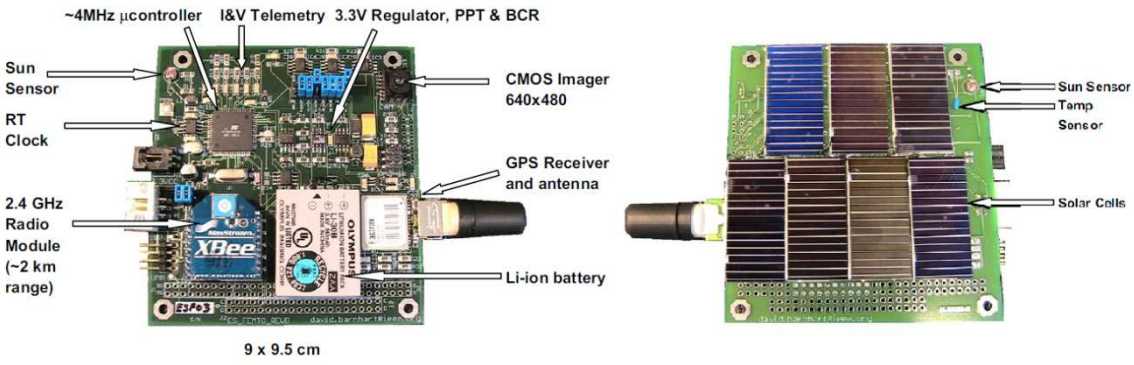

Figure 1.6 Surrey University's PCBSat (courtesy of University of Surrey)

The power subsystem is based on seven hobbyist solar cells, each costing $5 (in 2008). The efficiency of these cells is a modest 15%, and the power produced by the

set of seven solar cells is about 1.3 W. A Li-ion secondary battery was chosen; its capacity is 645 mA·h and would be used in eclipse and for peak power periods. To gather as much power as possible, this system used peak power tracking circuit (MAX 85679529.

The primary structure is based in a 4-layer PCB with the PC-104 form factor standard. The reason for this form factor is to be compatible with the EyasSat picosatellite simulator (www.eyassat.org).

Command and Data Handling is performed by a RISC microprocessor working at minimum frequency; the chosen chip was Atmel 128L, at 4 MHz clock speed, 4 kB SRAM, and 128 kB of flash storage. This choice is justified by to the high data rate requirements posed by a CMOS camera in the payload.

MaxStream XBee Pro was used for communication in the S band (2.4 GHz); the emitted power is 60 mW. It must be pointed out that in fact this transceiver is only useful for laboratory tests. If the mission is flown, the transceiver should be more powerful.

Attitude Determination and Control is performed with a GPS (iTrax 03-S) and cadmium sulfide light detectors located in the two faces of the femtosatellite for sensing the sunlight. A single axis magnetorquer is used for attitude control.

Thermal control is completely passive. Only the battery and the solar cells have temperature sensors to predict and evaluate their efficiency.

Chapter 2

STATEMENT OF THE PROBLEM

2.1 Interest of the problem

The thermosphere is the first region of the atmosphere found beyond the von Kármán line, and as such has a decisive influence in many phenomena. The dynamics of all the region is far from understood, and the presence of rather strong winds challenges many current assumptions of space science.

From a practical point of view, the lower thermosphere is one of the main uncertainties when determining the time and geographical coordinates for the re-entry of a satellite. Truly enough, the complex shapes of re-entering satellites (which have probably lost their attitude control, and can be broken) poses a great difficulty in this class of forecasts. But it is also true that the lack of detailed knowledge of the atmospheric conditions (especially density) add to this trouble. Thus, knowing the thermospheric properties through in-situ measurements in different solar conditions would be a valuable advantage to improve re-entry predictions.

Also, when a satellite is about to re-enter, it would be useful to launch a set of femtosatellites to the same orbit as the faulty satellite to obtain in-situ, real-time data to improve the re-entry estimate. The cost of this mission would be basically the launch cost (because it would require to be dedicated).

Despite its practical side, the main relevance of this mission is related to its scientific value. The thermosphere is a region of great importance for upper atmosphere studies, and its lower part is difficult to access. On the first hand, meteorological balloons fall short, the maximum height ever reached being just 53 km, scarcely over atmospheric midpoint to space; on the other hand, functional satellites are found at higher orbits (more than 300 km) to avoid early re-entry, and so no direct measurements are made in this region.

Then, the region between around 50 km and 300 km is difficult to directly probe. Our proposed femtosatellites could do so, over the whole Earth, during approximately a week. By launching swarms for different solar activity states, it could be possible to gather first-hand measurements to further improve our thermospheric models.

2.2 The Thermosphere

The region of the atmosphere of interest for this project is the thermosphere, and in particular the lower thermosphere, extending from the von Kármán line at 100 km to 250–300 km above sea level. As it has been stated before, above 300 km there is an important amount of active satellites –including the *International Space Station*– and

deploying a swarm of hundreds or thousands of femtosatellites would pose an unacceptable risk of collision, even if the residence time in these orbits would be of only a few months.

In what follows, we will succinctly describe the main characteristics of the thermosphere. This layer of the atmosphere extends from 85 km to 500 km of height, thus being over the mesosphere and below the exosphere. The lower altitude is fairly constant, but the higher is much more variable due to changes in the solar activity (the criteria to define the frontier between the exosphere and the thermosphere is that gases in the exosphere have enough kinetic energy to scape to space; this, naturally, depends on the kinetic energy of the constituents, as well as on their mass: the higher mass constituents need correspondingly higher kinetic energies to be lost into space).

As the name indicates, the thermosphere constituents are at a very high (kinetic) temperature due to the absorption of solar (mainly UV) radiation. This also causes the apparition of ionic species due to the loss of some electrons from the atmospheric gases. The ionosphere, in fact, encompasses the whole thermosphere, approximately extending from 60 to 600 km in height.

Thermosphere models allow the determination of temperature and density of this region as a function of location (latitude, longitude, and altitude), solar time, day-of-the year, and solar and geomagnetic activity.

Due to the absorption of solar radiation (the thermosphere is responsible of the largest fraction of absorbed radiation by the atmosphere), the temperature increases with height and is fairly variable, depending on the solar activity state. A reasonable approximation for the tropospheric temperature (that will be responsible for the kinetic energy of constituents) is [7]

$$T_\infty = 500 + 3.4\, F_{10.7} \qquad \textbf{(2.1)}$$

where the temperature is given in kelvin, and $F_{10.7}$ is the solar radiation at 10.7 cm wavelength measured in units of 10^{-22} W m^{-2} Hz^{-1}, (that is 10^4 jansky) which is the standard proxy for solar EUV (Extreme UV) radiation. This last factor is a measurement of solar activity, and ranges from 70 (quiet sun) to 250 (heavily perturbed sun); thus, the thermospheric temperature predicted by this model ranges from 750 to 1850 K. It must be recalled that the model temperature is just an approximation to real conditions.

The thermosphere is also heated by geomagnetic activity, which is measured by the daily geomagnetic index A_p. This index varies from 0, very quiet, to 400, which corresponds to a heavily disturbed terrestrial magnetic field. A value over 30 indicates some local geomagnetic disturbances.

Currently, it is not possible to forecast these two indexes, but only to give general trends based on rough predictions of solar activity. And even these general trends are sometimes far off the mark.

The end of the turbosphere, the region of the atmosphere in which chemical constituents are well mixed, is located at a height of around 110–120 km, thus being inside the thermosphere. This implies that most of the thermosphere is not well mixed, and that their constituents distribute in strata. The main thermospheric constituent is atomic oxygen, resulting from the dissociation of ozone and oxygen molecules by the UV light coming from the sun; minor components also found are H, He, N, N_2, O_2 and Ar.

As the density is not too low, it can be expected that the constituent species are near thermal equilibrium in the part of the lower thermosphere of interest in this Master Thesis. This makes possible to use standard kinetic gas theory to predict and interpret the physical conditions of the gas and plasma. In particular, the energy distribution of the atmospheric constituents follows a Maxwell-Boltzmann distribution.

There are several atmospheric models that include the thermosphere. During this Master Thesis we have employed the NRLMSISE-00 model [8]. This model includes, besides temperature and composition data, observed drag values measured from a range of satellites. This makes it preferable to Jacchia models, which are based just on satellite drag measurements obtained in the 1960s. The main contenders for NRLMSISE-00 are the model by Jacchia-Bowman [9], and DTM 2013 (see below). We plan to use them together with NRLMSISE-00 in future work as they could be preferable for determining total mass densities for altitudes above 120 km. NRLMSISE-00 is more accurate in the determination of temperature and composition of the thermosphere.

NRLMSISE-00 data have been gathered mainly with a Mass Spectrometer and Incoherent Scatter Radar for the last 50 years, giving the model an extremely sound foundation. Thus it is the usual standard for detailed orbit prediction, or forecast of re-entering space objects.

It must be stressed that in fact density is modified by several factors. One of the most relevant is atmospheric tides due to the solar irradiance, which has a limited impact in energy transport in the thermosphere; the second relevant factor are internal gravity waves, that account for a 250 K increase in the thermospheric temperature given by (2.1).

A further complication arises from the existence of winds with velocities of a few 100 m/s. The origin of the winds, as well as their dynamics are still a subject of intense study. The Horizontal Wind Model [10][11][12][13] is a reasonably realistic approximation, and includes solar and geomagnetic effects. As will be explained, the existence of these winds will require sets of femtosatellites injected into identical orbits, but with a subset in a prograde and the other in a retrograde orbit.

One of the newest models is the DTM (Drag Temperature Model) 2013, and it is worth commenting upon its improvements as compared with previous models. First, they have substituted the $F_{10.7}$ index by the F_{30} index, similar to the previous one, but determined at a wavelength of 30 cm, instead of 10.7 cm. The other improvement is highly relevant for this Master Thesis, as it consists in the inclusion of GOCE data gathered at 270 km of altitude. GOCE (Gravity field and steady-state Oceanic Circulation Explorer) was an ESA satellite devoted mainly to the precise

determination of the gravitational field of our planet. It was in a very low Earth orbit, at just 270 km above sea level, and its measurements required a disturbance-free environment. To cope with drag, the shape of GOCE was aerodynamic, arrow-like, and it had an ion engine that countered the deceleration caused by drag. As a by-product of the mission, GOCE determined with exquisite accuracy the density of the thermosphere at its operating altitude. The improved data has helped to significantly improve the accuracy of thermospheric models. This is, albeit with lower accuracy, the task that is charged to our swarm of femtosatellites. While our detectors are much cruder than GOCE's, our fleet would chart the region just below the orbit of GOCE up to the von Kármán line, and would probably result in an improvement of models.

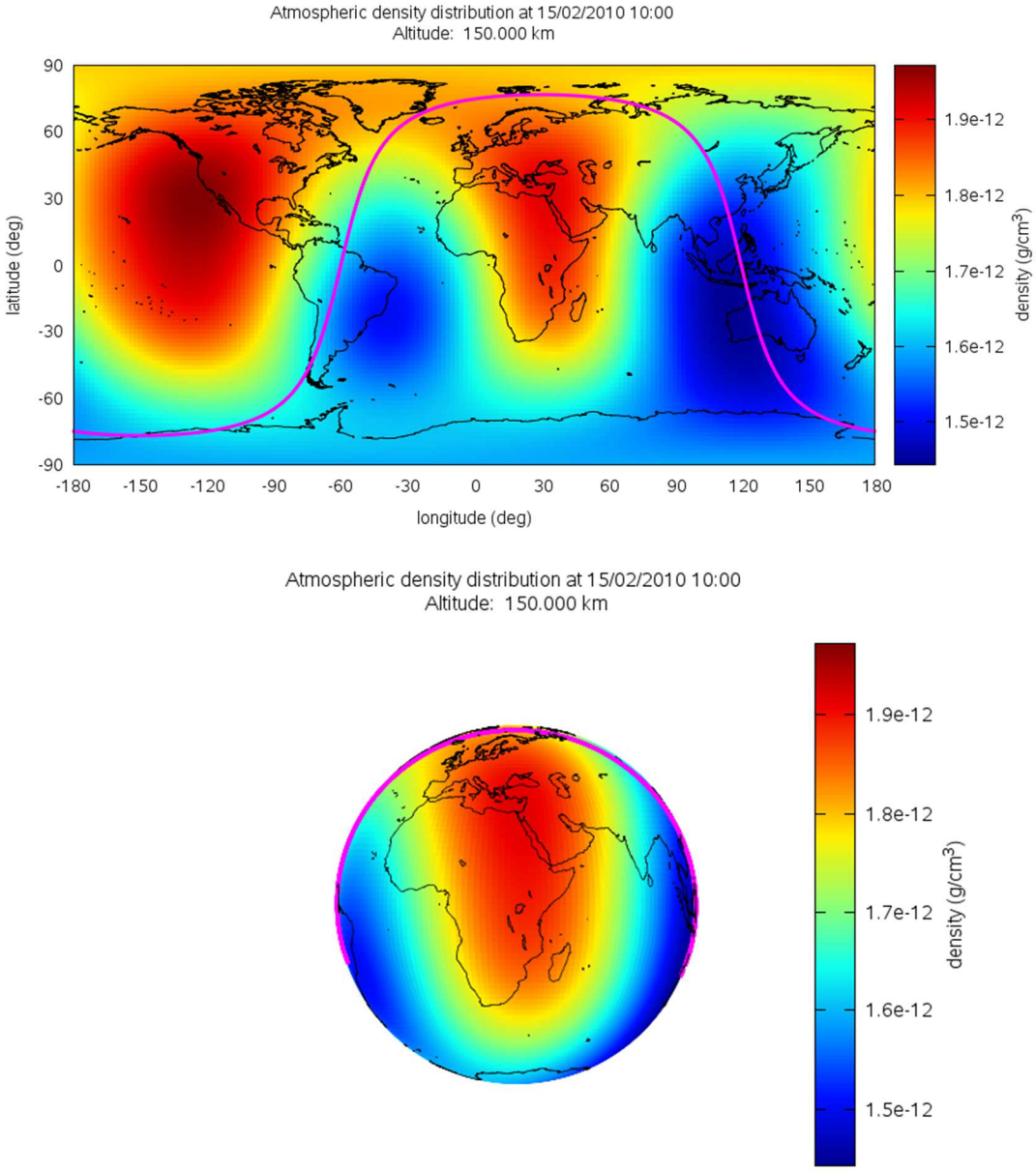

Figure 2.1 Density of the thermosphere at 150 km of altitude determined with the DTM2013 thermospheric model. The sun is shining over our hemisphere. In the day for which the calculations were made $F_{10.7}$ = 150

DTM 2013 is a semi-empirical model developed by CNES that determines the density, composition and temperature of the thermosphere in all conditions and locations. It employs F_{30} as a better proxy for solar activity, and especially for a much better prediction of solar EUV radiation intensities, than $F_{10.7}$, but this last index is also kept to allow comparisons with other models and historical data.

DTM 2013 is freely distributed at [14].

Chapter 3

MISSION OVERVIEW AND REQUIREMENTS

This chapter will give a general layout of the mission, and will derive some requirements that must be accomplished by the femtosatellite design. It will also describe some of the fields were more work must be laid upon to achieve a complete phase A analysis.

3.1 Mission Overview

The goal of this mission is to measure in a direct way the density of the lower thermosphere between the von Kármán line (100 km, the legal frontier between the air space and space itself) and an altitude less than 300 km. The upper limit is chosen not to be uncomfortably close to the International Space Station, which can be found at altitudes as low as 350 km. On the other hand, even the limit of 300 km is quite optimistic, as current technology MEMS accelerometers allow us to get data up to a height of about 220 km (for further details, see the description of the accelerometer in chapter 4).

Determining the density of the thermosphere in just one orbital path (using then just one femtosatellite) would be of rather limited interest. Our proposal plans to send a swarm of femtosatellites in different orbital alleys to cover the whole Earth with a resolution of a few hundred kilometres (which can be improved if more satellites are deployed). To gain whole Earth coverage, the orbits will be polar (inclination around 90 degrees), which will also be convenient for downlinking the data to high latitude ground stations.

Launching the swarm is an issue of considerable difficulty that merits a dedicated future study. We will just mention that putting the satellites in different orbital alleys would probably require separate launches. As there is no dedicated launcher for small masses (up to 100 kg, for example), this would call for a coordinated series of piggyback launches that look improbable.

Another possible caveat of the mission is related to orbital debris. There are two points to be stated in this regard. The first is that this region is almost devoid of functional satellites, as the altitude is that low that the re-entry would be a matter of weeks, at most. And this is precisely the second point: once deployed, the lifetime in orbit of our femtosatellites is very short, one to two weeks, depending on the solar activity state. Thus, even if launching a swarm of several thousand femtosatellites was feasible, its contribution to the space debris problem would be negligible. Nevertheless, this problem will also be thoroughly addressed on further works.

The envisioned femtosatellites will be spherical, and with a radius of 5 cm and a mass below 100 grams (otherwise, them would not be femtosatellites). To determine the air density the satellites will use the acceleration caused by the drag:

$$D = \frac{1}{2}\,\rho v^2\,S\,C_D = m\,a \qquad (\mathbf{3.1})$$

Then, the acceleration will depend directly on the atmospheric density (ρ), which is precisely the quantity to be determined, as well as on the square of the velocity relative to the atmosphere (v), the cross section (S), and the drag coefficient (C_D). Despite its apparent simplicity, the last equation holds many complications.

Determining the cross section is quite straightforward, as it is just the surface of a circle of radius 5 cm. But the other two terms hide considerable subtleties. On the first hand, the velocity is relative to the atmosphere, and then it will be similar –but not equal– to the orbital velocity with respect to the centre of the Earth. In our case, this orbital velocity ranges from 7.851 km/s at 100 km of height, to 7.779 km/s at 220 km. However, this velocity is just a part of the relative velocity, as the lower thermosphere is subjected to winds that can move at a significant speed (up to a few hundreds of meters per second). As we cannot forecast their velocity nor heading, we will have to deal with their effect in a different way. We have envisioned launching subsets of femtosatellites in orbits which are identical in all their orbital elements, except in the inclination, making the orbit of one of these subsets prograde, and the orbit of the other subset retrograde. In this way we will be able to determine the effects of winds as long as the distance between the subsets is not too large (as the winds are regional). Another way to deal with this problem is through data analysis of the complete mission, but here some assumptions must be made, which are always disputable.

On the other hand, the calculation of the drag coefficient is quite entangled, and plagued by several physical uncertainties. For the region of interest, a spherical object will have a drag coefficient of $C_D \approx 2.2 - 2.6$. This factor merits a detailed description which is presented in the next section.

With all these data in hand, and knowing that the typical atmospheric density at 150 km is of the order of 10^{-12} g/cm^3, we can determine an order of magnitude for the acceleration that must be measured:

$$a = \frac{1}{2}\,\rho v^2\,\frac{S\,C_D}{m} \qquad (\mathbf{3.2})$$

which results in an acceleration of ≈5.5×10^{-3} m/s^2. At the density corresponding to 250 km, around 5×10^{-14} g/cm^3, the resulting acceleration is just around 2.8×10^{-5} m/s^2. This is near the limit that can be measured with current MEMS accelerometers.

Each femtosatellite will be equipped with three single-axis accelerometer positioned at right angles, in order to measure the total acceleration experienced by the satellite. Besides that, a MEMS GPS will fulfil the tasks of positioning and time tagging the acceleration measurements. These measurements will be stored in a solid state memory, and packaged for transmission by the on-board computer. The transmission

times will be selected by determining the distance to a set of ground stations using the data from the GPS. All the system will be solely fed by a primary battery; due to the shape of the satellite and the aggressive environment, solar cells are not an option. The mass of the battery amounts for most of the total femtosatellite mass, and enables a mission duration similar to the decay time. To obtain the spherical shape, as well as for thermal control issues, the active part of the satellite will be embedded in a spherical piece of aerogel, which will be covered by a thin layer of a suitable space-qualified plastic if required.

To avoid problems due to the existence of a preferential rotation axis, we will design our spherical femtosatellite in such a way that all the principal inertia moments are equal (spherical top). We will also demand that the centre of mass is located in the geometrical centre of the sphere. Otherwise, pressure forces would cause a complex dynamic motion of the satellite.

3.2 C_D calculation

The drag coefficient (C_D) calculation is a central factor for the determination of the thermosphere density. Then, for a preliminary design, it has been used three different analytical methods in order to calculate the C_D. These are Schamberg's model, an alternative method to calculate quasi diffuse drag coefficients for simple geometries (in our case a sphere), and Cook's model. Nevertheless, in the final design of the femtosatellite, it is going to be used just one of these three models. The decision about which one to use is still to be made.

Several complications add in the determination of the drag coefficient, but the most relevant is the problem of the accommodation factor, which is not yet solved. When a particle impacts on an object, current wisdom assumes that it is reflected by the objects surface following the reflection law similar to that of geometric optics (that is, the incidence angle is equal to the reflection angle). However, this is not true for a fraction of the impacting molecules or ions.

Depending on the properties of the surface, on its temperature, and on the nature of the impacting particle, there is a significant probability that it gets stuck on the surface. The residence time of the particle on the surface depends mostly on the surface temperature: the lower the temperature, the longer the residence time. Once the particle stuck on the surface, it can be re-emitted in any direction, in what is called a Lambertian distribution. Thus, the exchange of linear momentum is different from classical elastic collisions. Most of the efforts of the theoretical models presented deal with this accommodation factor.

3.2.1 Schamberg's model

Regarding the Schamberg's model, it consists of a general gas-surface interaction model (GSIM), where after hitting the surface of a certain body the molecules are reflected with the scattering pattern of a half cone. In order to solve the problem, first of all, it has to be calculated the accommodation coefficient (α) by means of the equation (3.3), where E_i and E_r are the incident and reflected energy fluxes,

respectively, and E_w is the energy flux that would be taken away if all the molecules were reflected diffusely in thermal equilibrium with the surface of the body.

$$\alpha = \frac{E_i - E_r}{E_i - E_w} \tag{3.3}$$

Then, we can relate the velocity ratio (r) with the accommodation coefficient, as we can see in the equation (3.4).

$$r = \sqrt{1 - \alpha} \tag{3.4}$$

The function $\phi(\phi_0)$ characterizes the shape of the reflected beam, as it is showed in equation (3.5), where the term ϕ_0 is the cone angle.

$$\emptyset(\emptyset_0) = \frac{1 - \left(\frac{2\emptyset_0}{\pi}\right)^2}{1 - 4\left(\frac{2\emptyset_0}{\pi}\right)^2} \cdot \frac{\frac{1}{2}\sin 2\emptyset_0 - \left(\frac{2\emptyset_0}{\pi}\right)}{\sin \emptyset_0 - \left(\frac{2\emptyset_0}{\pi}\right)} \tag{3.5}$$

Finally, the drag coefficient it can be calculated by means of the equation (3.6), where the term f is the fraction of molecules reflected diffusely.

$$C_D = 2[1 + \emptyset(\emptyset_0) r f] \tag{3.6}$$

3.2.2 Alternative method

In order to calculate the drag coefficient, it also can be used an alternative method which consists of a simplification of the Schamberg's model for quasi diffuse drag coefficients of simple geometries like a sphere, as we can see in the equation (3.7).

$$C_D = 2\left(1 + \frac{4}{9} r\right) \tag{3.7}$$

3.2.3 Cook's model

It has been used the last model, which is the Cook's one. First of all, it is needed to calculate the E_w/E_i ratio by the equation (3.8), where T_w and $T_{k,i}$ are the wall and kinetic temperature, respectively.

$$\frac{E_w}{E_i} = \frac{T_w}{T_{k,i}} \tag{3.8}$$

Then, it can be calculated the velocity ratio, as we can see in the equation (3.9).

$$r = \sqrt{1 + \alpha\left(\frac{E_w}{E_i} - 1\right)} \tag{3.9}$$

Finally, the drag coefficient can be calculated by means of the equation (3.10).

$$C_D = 2\left(1 + \frac{4}{9}r\right) \qquad (\mathbf{3.10})$$

3.3 Mission requirements

From the above analysis we can derive several requirements for the individual femtosatellite. A swarm of femtosatellites would have to fulfil these requirements, as well as some related to the orbital structure of the fleet, and to the launch and orbital insertion.

The femtosatellites shall

1. Be able to measure in real time accelerations as small as 10^{-5} m/s^2 (10^{-6} g)
2. Have an inertia tensor of the spherical top form ($\{I\} = K\{Id\}$), and the centre of mass must be located at the geometrical centre of the sphere
3. Be able to precisely determine its location and the time
4. Have a life expectancy of one week
5. Be capable of downlinking the scientific data gathered
6. Not cause a significant debris risk for other satellites in LEO
7. Passively control the temperature inside the operational margins marked by the payload
8. Resist the stress of the launch

Chapter 4

PRELIMINARY DESIGN

In this chapter we will discuss a preliminary design intended to fulfil the set of requirements listed in section 3.3. First, we present the choice of electronic devices chosen to construct the femtosatellite, and afterwards we briefly discuss the primary structure.

4.1 Electronic components

It is important to highlight that all the electronic components which we have chosen in order to do the preliminary design of the femtosatellite consists of commercial off-the-shelf (COTS) products. Furthermore, we have done an exhaustive research and a proper selection of all these components to achieve four essential characteristics for our satellite: reduced size, small mass, low power consumption and reduced cost. Hence, the payload of the femtosatellites would consist of three single-axis accelerometers, a microprocessor, a GPS, a flash memory, a transmitter (with an omnidirectional dipole antenna), two voltage regulators, and a primary battery.

4.1.1 Accelerometers

Regarding the system of accelerometers, it is necessary to mention that these electronic components are the most important ones of the payload and for the fulfilment of the mission. With them it will be possible to determine the density in the thermosphere, after determining the acceleration experienced by the femtosatellite along its orbit.

Then, we have chosen the model 8330A2.5 ServoK-BEAM of Kistler®, which highlights itself for its high sensitivity (1500 mV/g) and resolution (0.8 μg). Furthermore, it has an acceleration range of ±2.5 g_{pk} and a shock rating of 1500 g_{pk}. Respecting its electrical characteristics, the accelerometers have an operation voltage range of 6-15 V and their nominal current is 8.5 mA. Moreover, the operating temperature range goes from –40 to +85 ºC.

The sensor and conditioning circuits are integrated into an epoxy sealed aluminum housing, which would be removed in order to reduce considerably the total mass of the femtosatellite, and thus maintaining our design inside the specific mass range for this category of satellites.

Moreover, the sensing element consists of a three terminal silicon micro-machined variable capacitance sensor of 10x10x3 mm, and has a total mass of 2 g. This sensor provides excellent bandwidth, dynamic range, stability, and robustness, and it is made using MEMS (microelectromechanical systems) technology.

The three accelerometers would be attached together, in such a way that they would be oriented to determine the acceleration in the three axes (X, Y and Z). Then, determining the total acceleration would be a simple modulus determination, and completely independent of the orientation of the satellite. It is interesting to note that 3-axis MEMS accelerometers already exist in the market, but their sensitivity is worse than what we need, and the Z axis is plagued with a lower sensitivity than the other two, thus making important to determine the orientation of the femtosatellite (something that our femtosatellite, due to its simplicity, is not able to do). Both reasons were sufficient to prefer the, apparently more clumsy, solution based on three one-axis accelerometers.

It is important to mention that this model of accelerometer has been chosen carefully among many others, because it is suitable for applications that require measurements of low acceleration as well as being small and light. Because of its outstanding performance features, this accelerometer is perfect to replace traditional accelerometers in several specific applications, such as vibration control for optical or precision manufacturing processes, platform levelling (pitch and roll measurements), high speed trains (tilt and lateral vibration measurements), measuring seismic events on structures (earthquakes), and general vibration for automotive dynamics. And also for out femtosatellites.

Figure 4.1 shows one of the accelerometers together with its aluminum housing.

Figure 4.1 Commercial version of the chosen accelerometer

Table 4.1 shows a list containing extra technical features of this device, which has been directly extracted from its datasheet.

Table 4.1 Technical data for the chosen accelerometer

Technical Data Type		Units	8330A2.5
Acceleration Range		g_{pk}	±2,5
Sensitivity (Scale Factor) ±5 %		mV/g	1500
Zero g Output ±300mV		V	0
Resolution (Threshold) typ. (0…10 Hz)		µg	< 2,5
Amplitude Non-linearity		%FSO	± 0,2
Resonant Frequency nom.		Hz	5000
Frequency Response	±5%	Hz	0 … 300
	±3dB	Hz	0 … 2000
Noise Density (0…100 Hz) typ.		$\mu g_{rms} / \sqrt{Hz}$	0,8
Phase Shift max.	@ 0 Hz	degree	0
	@ 100 Hz	degree	1
	@1000 Hz	degree	5
Sensitive Axis Misalignment typ. (max.)		degree	<0,4 (0,8)
Transverse Sensitivity typ. (max.)		%	0,4 (1)
Environmental:			
Random Vibration 20… 2000 Hz		g_{rms}	20
Shock half sine, 500µs		g_{pk}	1500
Temperature Coefficient of:			
Sensitivity typ. (max.)		ppm/°C	50 (100)
Bias typ. (max.)		µg/°C	100 (200)
Temperature Range Operating		°C	–40…85
Temperature Range Storage		°C	–55…125
Output Impedance		Ω	< 40
Load Resistance min.		kΩ	5
Capacitive Load max.		pF	10000
Supply: (bipolar)			
Voltage		VDC	±6 … ±15
Current nom.		mA	8,5
Construction:			
Sensing Element		type	MEMS
Housing/Base		material anodized	Al. hard
Sealing - housing/connector		type	Epoxy
Connector		type	4-pin pos. Microtech Equivalent
Ground Isolation min.		MΩ	10
Weight		grams	28,5

4.1.2 Microcontroller

Regarding the microcontroller, it will be in charge of processing all the data that come from the sensors, packetizing them, and sending them to the transmitter for downlinking; it will be also tasked with controlling all the peripheral devices to ensure their proper performance during the whole mission. Another task for it will be that of determining the periods of downlink by computing the distance to the ground stations used for the mission. This will be made by using the on-board gathered GPS data and the list of geographical locations of the ground station network.

The microprocessor which would be used is the model PIC18F1XK22 of Microchip®, which consists of an 8-bit high performance microcontroller of 20 pins (17 I/O pins and 1 Input-only pin) with small size (6x6x0.95 mm) and light weight (3 g). In addition, it is important to mention that it can operate up to 16 MIPS, which will be more than enough for our needs. Regarding its electrical features, the microcontroller has an operation voltage range of 2.3-5.5 V, and its nominal current is 25 mA. The operating temperature range of thus device goes from –40 to +125 ºC.

As regards the organization memory of this microprocessor, there are three types of memory, which are the program memory (up to 16 kbytes), data Random Access Memory or RAM (up to 512 bytes), and data Electrically Erasable Programmable Read-Only Memory or EEPROM (256 bytes). The data and program memory use separate buses, which allows the simultaneous access of the two memory spaces.

The program memory can be readable, writable and erasable during normal operation processes. A read from program memory is executed one byte at a time, whereas a write to program memory is executed on blocks of 16 bytes at once. Furthermore, this memory type is erased in blocks of 64 bytes at a time.

The data memory in this microcontroller is implemented as static RAM. This is an advantage, as SRAM is more resistant to single event upsets caused by ionizing radiation than is standard RAM. Each register of the RAM has a 12-bit address, in such a way that it allows up to 4096 bytes of data memory. In addition, the memory space is divided into a maximum of 16 banks which contain 256 bytes each one.

The data EEPROM is a nonvolatile memory array, which is separated from both the data RAM and the flash program memory, and is used for long-term storage of program data. Moreover, the data EEPROM is readable and writable for normal operation process. Nevertheless, we do not plan to give the femtosatellites a reception capability, and so this last property will be of no use.

Although the internal memory capacity is quite small, we are going to use a lossless algorithm (yet to be chosen) in order to compress all the data generated by the payload before storing it in the external flash memory. As we will see in section 5.1, nevertheless, the amount of data gathered is relatively small.

The oscillator module consists of three different clock sources and has several features which allow using it in a wide range of applications, improving the performance of the device and reducing the total power consumption (this aspect is important to increment the total battery life of the femtosatellite). The three clock

sources that constitute the oscillator module are: a primary external oscillator (up to 64 MHz), a secondary external oscillator (up to 32 kHz) and the precision internal oscillator (up to 16 MHz). In addition, this microcontroller can work with 13 different oscillator modes, which may be programmed by the user.

As regards the Analog-to-Digital Converter (ADC), it is the responsible of carrying out the conversion of an analog input signal to a digital one. This has a resolution of 10 bits and consists of 12 different channels. Moreover, it is important to highlight that the ADC module can work even during the Sleep mode. As the data from the accelerometers and the GPS will already be digital, the ADC will have no use for the mission.

The main characteristic to highlight is its low power consumption due to several power-managed modes that it provides. This is the main reason why we have chosen this microcontroller among many others. There are three different categories of power-managed modes, which are the following ones: Run modes, Idle mode, and Sleep mode. These three categories determine which portions of the microcontroller are clocked and at what speed. The Run and Idle modes can use any of the three available clock sources, whereas the Sleep mode does not use any clock source. In our case, we are going to use one of the Run modes, which is the one called RC_Run mode. In this mode, clocks to both the core and peripherals are active, and it provides the best power conservation of all the Run modes.

In figure 4.2, we can see a schematic of the microprocessor, where all its pins are numerated and named.

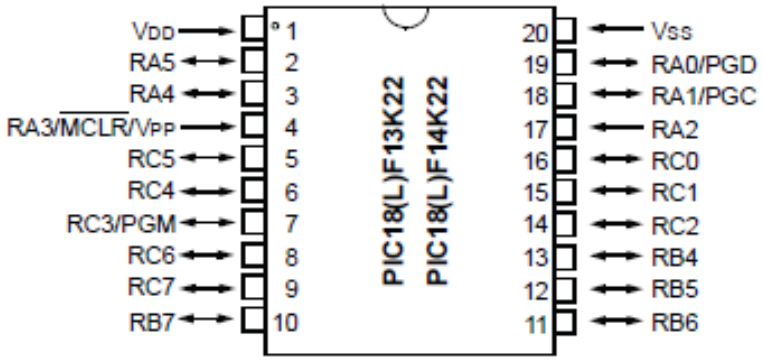

Figure 4.2 Pin map of the microcontroller PIC18F1XK22 of Microchip®

4.1.3 GPS receiver

Regarding the GPS receiver, it will be the device in charge of fulfilling the tasks of positioning and also time tagging the acceleration measurements.

As GPS receiver, we will use the model MAX2769 of Maxim Integrated®, which is the first industrial Global Navigation Satellite System (GNSS) receiver that provides GPS, GLONASS, and Galileo navigation in a single chip. It highlights itself for its small size, because it is packaged in a 5 mm x 5 mm thin package of 28 pins, and

has a tiny mass of just 1 g. Moreover, the total cascade noise figure of this device is as low as 1.4 dB.

Given the configuration of our femtosatellite, and its small size, we do not expect any multipath problem. Even if they appear, its impact on the mission will be completely negligible.

Respecting its electrical features, the GPS receiver has an operation voltage range of 2.7-3.3 V and its nominal current is 15 mA. The operating temperature range goes from –40 to +85 ºC.

In addition, we can remark that the MAX2769 is one of the most flexible receivers on the market, because the integrated frequency synthesizer allows programming in the IF frequency with a ±40 Hz accuracy, whereas it operates with any reference or crystal frequencies that are available in the host system.

The device incorporates the complete receiver chain, adding a dual-input LNA and mixer, followed by the image-rejected filter, PGA, VCO, fractional-N frequency synthesizer, crystal oscillator, and a multibit ADC.

This GNSS receiver does not need the use of external IF filters by implementing on-chip monolithic filters, and requires just a few external components in order to form a complete low-cost GPS receiver option.

It is important to mention that this GPS receiver is subjected to the “CoCom (Coordinating Committee for Multilateral Export Controls) limits”; according to it the receiver should disable tracking when the device is moving faster than 1000 knots (1900 km/h), and/or at an altitude higher than 60 000 feet (18 000 m). The implementation of this measure helps to avoid the use of GPS in ballistic missiles. Then, the manufacturer of the receiver should change the device software (firmware) in order to use it in our femtosatellite, after demonstrating that we are part of a peaceful organization.

Furthermore, it is important to take into account that this device has a low-power mode by programming the pertinent bias current values of each block that constitutes the receiver to their minimum values. By means of this mode, the current of all receiver blocks are reduced to the minimum recommend values, as well as the bias antenna circuitry is totally disabled (this is not an important problem for the proper performance of the femtosatellite during the mission). Moreover, with this mode the total current is reduced to just 10 mA. Nevertheless, the total cascade noise figure would be increased to 3.8 dB.

In figure 4.3, we can see this model of GPS receiver.

Figure 4.3 Maxim MAX2769 GPS receiver

4.1.4 Flash memory

The flash memory will be the device in charge of storing all the data generated by the sensors and processed by the microcontroller, before sending it to the ground station.

Hence, we are going to use the model PC28F00AG18xx of Micron®, which has a memory capacity of 1 Gb with eight partitions of 128 Mb. In addition, it provides high read, write and erase performance at low voltage (1.7 V) with a 16-bit wide data bus. As regards to its electrical features, the flash memory has an operation voltage range of 1.7-2 V and its nominal current is 23 mA. The total mass of the device is just 1 g and its operating temperature range goes from –30 to 85 ºC.

The most relevant features of this device about quality and reliability are: the provision of a minimum 100 000 erasable cycles per block and the use of 65 nm process technology in order to build this flash memory model. To qualify it for the mission, it will be necessary to make some radiation tests using a cobalt source.

Another important characteristic to highlight is that it has a one-time programmable (OTP) space, which is quite useful for security matters. The OTP space provides 2112 user-programmable OTP bits and has 64 unique factory device identifier bits.

The multi-partition architecture that it presents, provides read-while-write and read-while-erase capability, with individually erasable memory blocks sized for optimum code and data storage. Furthermore, it is important to mention that this device has power savings features, including an automatic power savings mode, a standby mode, and a deep power-down mode.

With respect to the automatic power savings mode, it provides low-power operation carrying on reads during active operating mode. Once the data is read from the memory array and the address lines are inactive, this mode automatically sets the device into standby. In addition, the automatic power savings can reduce the operating device current to just 60 µA.

Moreover, it is important to highlight that this flash memory has been designed especially for applications areas that require a low voltage.

In figure 4.4, we can see an illustration of the flash memory.

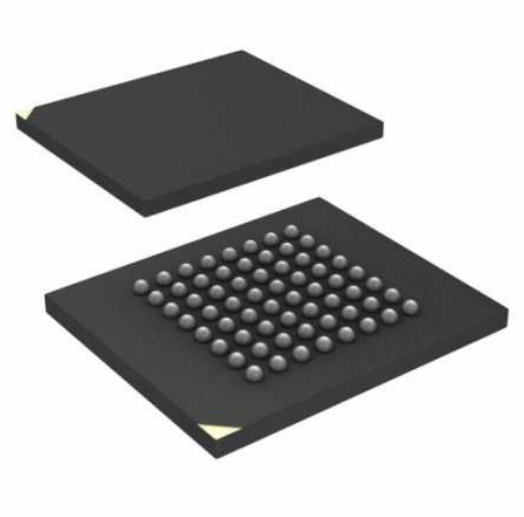

Figure 4.4 Flash memory

4.1.5 Transmitter

The mission of the transmitter is to carry out the delivery of data generated by the satellite, by means of a suitable antenna.

The transmitter which would be used is the model INST-11B of Syntronics®, which consists of a micro S-band transmitter of only 0.8 inches in diameter and a mass of 2 g. This device has a RF output of 0.33 W and its frequency can be varied from 2.205 GHz to 2.295 GHz in 500 kHz increments. Moreover, the input transmission range is between 500Kb/s and 2 Mb/s, depending on the specification of the user at the time of ordering it. As regards to its electrical features, the transmitter has an operation voltage of 3.3 V and its nominal current is 500 mA. The operating temperature range goes from –40 to +85 ºC.

It is also important to mention that this transmitter has been tested by many customers, and has been proven to be reliable in a gun launch environment of up to 20 000 G when it is properly mounted.

It is important to mention that this tiny transmitter is especially suitable for applications which require the integration of telemetry in a small system. Furthermore, we can highlight that all the S-band configurations are available with a three week typical, six week maximum, lead time from the receipt of order, which is quite a good time for this type of devices.

Moreover, it is going to be used together with an omnidirectional dipole antenna, which is suitable for our case because of the lack of attitude control of the satellite, in

order to send all the data generated by the femtosatellite to the ground station network.

In figure 4.5, it is shown the transmitter together with a directional patch antenna (not useful for our case) compared in size with a quarter dollar coin.

Figure 4.5 Transmitter INST-11B of Syntronics®

4.1.6 Voltage regulators

Furthermore, it would be used two voltage regulators with a mass of 2 g each one in order to feed both the three accelerometers and the transmitter (6 V), and the other to power the flash memory (1.7 V). The model used is the LM317 of Texas Instruments®, which consists of a 3-terminal adjustable regulator with an output voltage that can vary from 1.25 V to 37 V, and is able to supply more than 1.5 A. Its operating temperature range goes from –55 to +150 ºC.

In order to achieve a higher performance than fixed regulator models, this electronic component provides on-chip current limiting, thermal overload protection, and safe-operating-area protection. The overload protection remains working completely, even if the Adjust (ADJ) terminal has been disconnected.

It is important to mention that this model of voltage regulator is extremely easy to use, because it just requires two external resistors (R_1 and R_2) to set the output voltage, as we can see in figure 4.6.

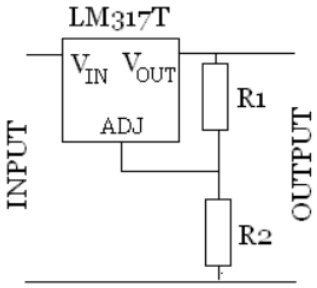

Figure 4.6 Circuitry for voltage regulators

Hence, we have calculated the resistors values for both cases, by means of the equation (4.1) and fixing the value of R_1 at 240 Ω, and V_{ref} = 3.6 V (voltage supplied by the primary battery). For a V_0 = 6 V and V_0' = 1.7 V, the values of R_2 are 160 Ω and 120 Ω, respectively.

$$V_0 = V_{ref}\left(1 + \frac{R_2}{R_1}\right) \qquad (\mathbf{4.1})$$

In figure 4.7, we can see one of the voltage regulators.

Figure 4.7 Voltage regulator LM317 of Texas Instruments®

4.1.7 Primary battery

Finally, as primary battery we are going to use the model ER26500 of EEMB® to feed all the electronic components of the femtosatellite. It consists of a Lithium/Thionyl Chloride Cylindrical battery (Li-Thionyl) of C size, with a nominal voltage of 3.6 V and a capacity of 9000 mAh. In addition, it is important to mention that this battery has a mass of only 55 g, which means that it possesses a high energetic density. The operating temperature range goes from –55 to +85 ºC.

Regarding other features of this battery, we can highlight that it has an outstanding shelf life (10 years at room temperature), low self-discharge (1% or less per year), and it is suitable for long-term uses with low current.

Furthermore, the ER26500 can be used in several applications areas, such as water meters, gas meters, kWh meters, electronic packing meters, PC real-time clocks, medical equipment, etc.

Figure 4.8 shows us this model of battery.

Figure 4.8 Battery ER26500 of EEMB®

4.1.8 Electronic components summary

In table 4.2, it is shown the main characteristics (operating electrical features, operating temperature range and mass) of all the electronic components which constitute the femtosatellite.

Table 4.2 Summary of physical properties of chosen electronic devices

Component	Voltage (V)	Current (mA)	Power (W)	Operating temperature (ºC)	Mass (g)
Battery	3.6	–	–	–55 to 85	55
GPS	2.85	10	0.029	–40 to 85	1
Flash memory	1.7	23	0.039	–30 to 85	1
Transmitter	3.3	500	1.65	–40 to 85	2
Accelerometer	6	8.5	0.051	–40 to 85	2
Microcontroller	3	0.6	0.002	–40 to 125	3
Voltage regulator	3.6	3.5	0.013	–55 to 150	2

As can be seen from the table, the total mass of electronic devices is just 66 grams, which gives ample margins for structure, and ballasts (see sections 4.2 and 4.3).

The most limiting case for thermal control will be the low temperature end of the flash memory, but in general all the components have ample margins for operational temperatures.

Finally, the total power consumption is 134 mW excluding the transmitter. The transmitter will be operational for only brief periods of time. Otherwise, this 1.65 W would drain our battery in a matter of a few hours.

4.2 Structure

All the electronic components, which have been previously mentioned, would be embedded in a sphere of silica aerogel with 10 cm of diameter that will be covered by a thin layer of a suitable space-qualified plastic. This external layer of plastic is in place to protect the aerogel and for thermal control purposes. The aerogel itself provides protection to the internal subsystems from both the aerodynamic heating and the effects of the atomic oxygen. Silica aerogel is a suitable material for the femtosatellite, due to its extremely low density (around 0.003 g/cm^3) and low thermal conductivity. It is important to mention that the total mass of the structure would be around 1 g.

Table 4.3 lists the most salient physical properties of silica aerogels. Taken from [15].

Table 4.3 Physical properties of silica aerogels

Property	Value
Apparent Density	0.003-0.35 g/cm^3
Internal Surface Area	600-1000 m^2/g
% Solids	0.13-15%
Mean Pore Diameter	~20 nm
Primary Particle Diameter	2-5 nm
Index of Refraction	1.0-1.05
Thermal Tolerance	to 500 C
Coefficient of Thermal Expansion	2.0-4.0 x 10^{-6}
Poisson's Ratio	0.2
Young's Modulus	10^6-10^7 N/m^2
Tensile Strength	16 kPa
Fracture Toughness	~0.8 kPa*m$^{1/2}$
Dielectric Constant	~1.1
Sound Velocity Through the Medium	100 m/sec

As can be seen from table 4.3, the mechanical and thermal properties of silica aerogel are very convenient for structure and thermal subsystems. Mechanically, despite its very low density, it sports a high mechanical strength, with a Young modulus over 10^6 Pa. Thermal conductivity is very low (typically around 17 mW/m·K), which makes this material a very good thermal insulator. Then, the excursions in temperature for the central part of the femtosatellite, where the active devices are housed, will be quite reduced.

In figure 4.9, we can see an example of sphere made of silica aerogel.

Figure 4.9 Sphere cast in silica aerogel

4.3 Inertia tensor modification

As will be recalled, requirement 2 of section 3.3 stated that the femtosatellite would have the inertia tensor of a spherical top; that is, an inertia tensor with all the products of inertia equal to zero, and all the principal inertia moments equal. Of course, we realize that in general this will not be the case, as the mass distribution will not be appropriate.

In this section, we are going to explain how to determine the inertia tensor of the femtosatellite, and how to modify it in order not to have a preferred rotation axis, and thus avoiding that atomic oxygen degrades just a part of the femtosatellite surface. This latter situation would introduce an uncertainty in the interaction between the atmosphere and the satellite (by the effects of surface roughness on the value of the drag coefficient).

We want to obtain an inertia tensor of this form: $I = k\mathbb{I}$ and we also impose the condition $\vec{R}_{\text{CM}} = \vec{0}$. In general, the real inertia tensor will have different inertia moments, and inertia products not equal to zero. It is a well-known theorem of Classical Mechanics that it is always possible to cancel the inertia products by using

a suitable reference system, which then is called reference system of principal axes. Hence, we will obtain this:

$$I_{principal} = \begin{pmatrix} I_X & 0 & 0 \\ 0 & I_Y & 0 \\ 0 & 0 & I_Z \end{pmatrix}, \text{ where } I_X \neq I_Y \neq I_Z \qquad \textbf{(4.2)}$$

If we add six masses along the principal axes (symmetrically disposed with regard to the centre of the principal axis system to avoid perturbing the condition imposed on the centre of mass' location) at a certain distance of the centre of mass, the femtosatellite will behave like a spherical top, in such a way that $I_X = I_Y = I_Z$.

We have employed a 3D CAD software (SolidWorks®) to model the femtosatellite in a simplified way, and thus being able to do an analysis of its physical properties, highlighting the inertia moments measured from the centre of mass. In figure 4.10, we can see the preliminary design of the satellite and the corresponding physical properties (most importantly, total mass, location of the centre of mass, and inertia tensor). It is important to mention that the aerogel-plastic structure has been considered as negligible at the time of modelling the femtosatellite in order to simplify both its design and the pertinent calculations. Nevertheless, given that it boasts spherical symmetry, the changes will be rather small.

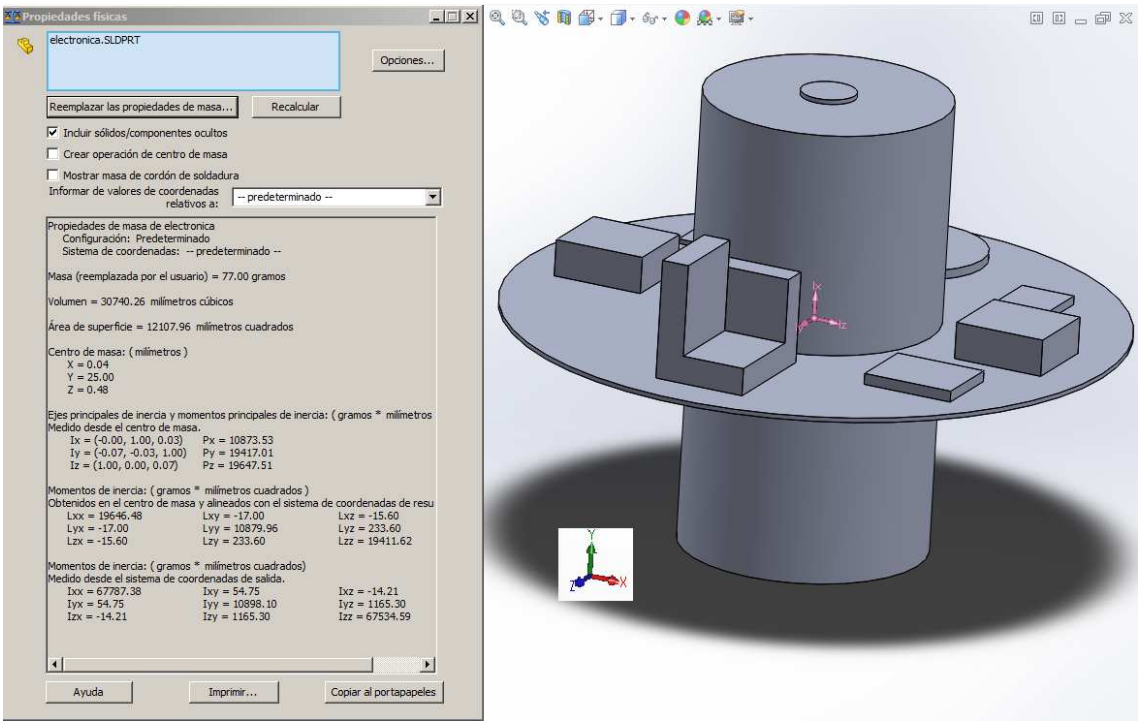

Figure 4.10 CAD realization of the femtosatellite design

To obtain the required form of the inertia tensor, we have added four spheres with a mass of 3.9 g (m_1) each one (to maintain the same centre of mass) symmetrically along the axis X and Z (see figure 4.11), placing them on the edge of the circular printed circuit board. In this way we have been able to considerably reduce the

difference between the three inertia moments. The mass of each sphere has been calculated by means of the equation (4.3).

$$I'_Y = I_Y + 2m_1r^2 \qquad (\mathbf{4.3})$$

In the following picture, the updated design of the femtosatellite and its physical properties are also shown.

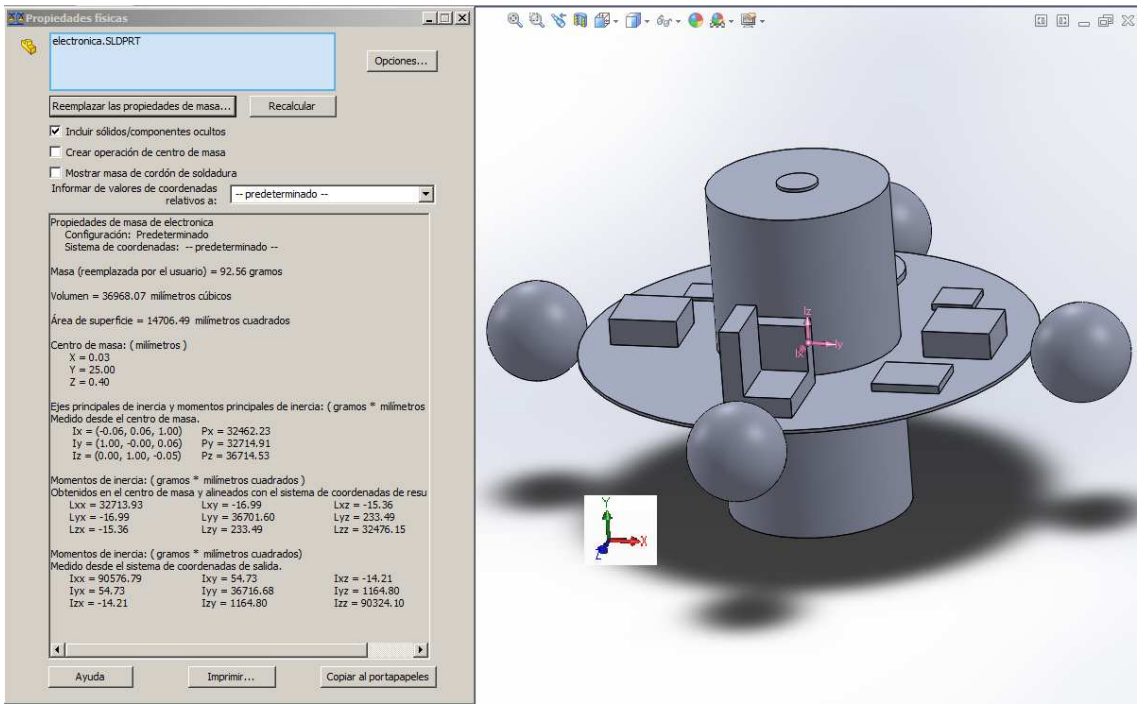

Figure 4.11 Design to reduce the difference between principal inertia moments

Finally, to obtain the spherical top inertia tensor we have added two extra spheres of the same mass (m_2=3.36 g) along the Y axis, placing them on the ends of the primary battery, in order to equalize definitely the three inertia moments. Hence, the femtosatellite would behave like a spherical spinning top, in such a way that it will not have a preferred rotation axis. The mass of each sphere has been calculated with the equation (4.4).

$$I'_X = I_X + 2m_2r^2 \qquad (\mathbf{4.4})$$

Again, in figure 4.12, we can see both the final design of the femtosatellite and its physical properties.

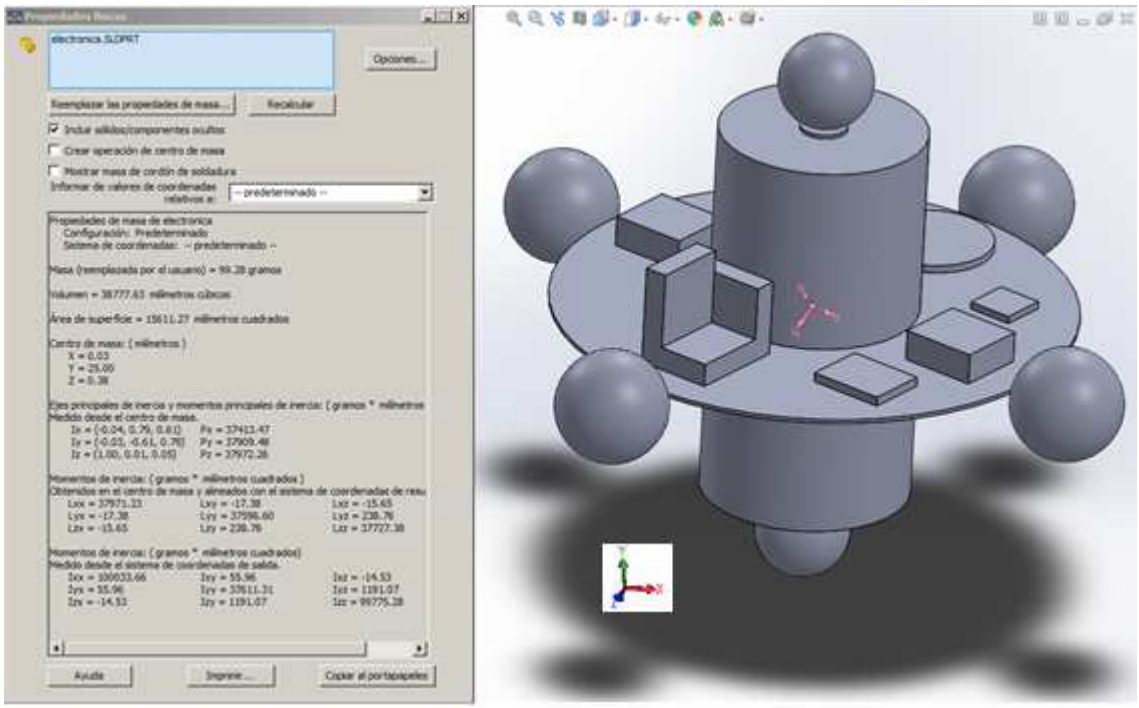

Figure 4.12 Final design of the femtosatellite fulfilling requirement 2 (centre of mass in the geometrical centre of the satellite, diagonal inertia tensor with equal inertia moments).

Chapter 5

MISSION ANALYSIS

One of the most relevant parts of a Phase A study as this consists in a general mission analysis. This must show that, at least to first order, the proposed design for the femtosatellite is able to comply with the requirements and drivers of the mission. In what follows we will discuss the main topics of mission analysis, the ones related to link design, electric power subsystem, and thermal control.

5.1 Data gathering

One of the main issues in a scientific mission as the one proposed is the data generation (or gathering) rate, as these data must be transmitted to ground stations without degradation (i.e., it cannot be compressed using lossy algorithms, which enable a greater compression than loss-less algorithms).

Thus, we have to determine the amount of data generated by orbit for each femtosatellite. This will be the main driver for the on-board mass storage system, as well as for the downlink transmitter.

For a reasonable resolution, we plan to obtain one measurement each second from each femtosatellite. Hence, for a 90 minute orbit, we will have 5400 measurements. Each measurement will be composed by the position and time (as given by the GPS), the acceleration (as given by the modulus determined through the individual measurements of the three single axis accelerometers), and a temperature reading (obtained by the temperature sensor integrated in the accelerometers).
The amount of bits gathered is (to first order) as follows:

1. Longitude: 32 bit (to 1 cm accuracy)
2. Latitude: 32 bit (to 1 cm accuracy)
3. Time: 24 bit (to 0.01 s accuracy)
4. Acceleration: 30 bit (to 10^{-9} m/s^2 accuracy)
5. Temperature: 17 bit (to 0.01 K accuracy)

This makes a total of 135 bits per measure. Adding some bits for satellite identification, orbital count, housekeeping, and message integrity issues, we can safely assume that the total amount of data per orbit will be of the order of:

$$N = (135 \times 5400) \times 1.2 + 500 \approx 900 \text{ kbit} \qquad \textbf{(5.1)}$$

The transmission data rate must be able to cope with this amount of data. To obtain a conservative estimate, we assume that we must downlink 1 Mbit of (uncompressed) data per orbit, and that the contact with the ground station can be maintained for two minutes. This gives us a data rate of about 8.5 kbit/s, or about 70

times lower than the lowest data rate of the chosen transmitter (500 kbit/s, see section 4.1.5)

$$R = \frac{10^6}{120} = 8.333 \text{ kbit/s} \quad \textbf{(5.2)}$$

which is below the maximum data rate that can be send by the chosen transmitter.

Now we can proceed with a preliminary analysis of the link (to do so, we closely follow [16]). The link equation is

$$\frac{E_{\text{bit}}}{N_0} = P + L_{\text{l}} + L_{\text{pr}} + L_{\text{a}} + L_{\text{s}} + G_{\text{r}} + G_{\text{t}} + 228.6 - 10 \log T_{\text{s}} - 10 \log R \quad \textbf{(5.3)}$$

For the transmitter we have that $\nu = 2.4$ GHz and then $\lambda = 0.125$ m. Using these data together with the ones given by the transmitter properties, we have:

$P = 0.2$ W $= -0.7$ dBW
$L_{\text{l}} = 0$ dB
$L_{\text{a}} = -0.3$ dB
$L_{\text{pr}} = -0.3$ dB
$L_{\text{s}} = -160.1$ dB
$G_{\text{t}} = 0$ dB
$G_{\text{r}} = 47$ dB
$T_{\text{s}} = 300$ K

In the last figures, we have assumed the use of ground system with a parabolic antenna of 10 m of diameter, and with an antenna efficiency of $\eta = 0.75$. Then

$$G_{\text{r}} = \frac{\eta \pi^2 D_{\text{r}}^2}{\lambda^2} \quad \textbf{(5.4)}$$

the spatial losses are given, assuming a contact distance of 1000 km, by

$$L_{\text{s}} = 147.55 - 20 \log d - 20 \log \nu \quad \textbf{(5.5)}$$

If we require a margin of 10 dB or 20 dB for our communications, we find that this allows data rates of 84 Mbit/s and 7.9 Mbit/s, respectively, which are orders of magnitude higher than our requirement. This ensures that we will have an excellent BER (Bit Error Rate).

The ground station network is still to be defined. However, considering that the orbits of the femtosatellites are almost polar, a group of small ground stations located at high latitude would suit perfectly the mission. The amount of data to be downloaded is not very high 900 kbit/orbit/satellite. Even if having a large number of satellites, two or three ground stations could easily cope with the downlink. To keep the cost of the ground station network low, we will design a software-defined-radio system. It is also possible to use some federation of ground stations, as Genso (which, despite being sponsored by ESA, seems to be stalled; for more information see [17]). Currently, there are several projects along this line of action.

5.2 Thermal control

One of the main issues with this class of satellites is thermal control as the limited power available on-board makes it necessary to employ only passive thermal control systems. Moving at so low altitudes poses special problems for thermal control, mainly due to the aerothermal heating and to the effects of the remaining atmosphere (due to sputtering and to the effects of atomic oxygen).

In our case of study, the equation of thermal balance is

$$A_{\text{sc}}\varepsilon\sigma T^4 = A_{\text{sun}}\alpha J_{\odot} + A_{\text{planet}}\alpha a J_{\odot} F_a + A_{\text{planet}}\varepsilon J_{\oplus} F_a + Q + Q_{\text{aerothermal}} \qquad \textbf{(5.6)}$$

where A_{SC} is the skin area of the satellite, A_{sun} and A_{planet} are the cross sections to the Sun and to the Earth, respectively, α and ε the optical absorptivity and infrared emittance, a the Earth's albedo (approximately 0.3), F_a the Earth's visibility factor of the Earth as seen from the orbital altitude (about 0.95), $J_{\odot}$ and $J_{\oplus}$ the power fluxes of the Sun (mostly visible, 1376 W/m^2) and the Earth (infrared, 237 W/m^2), and finally, Q is the power dissipated in the satellite, and $Q_{\text{aerothermal}}$ represents the aerothermal heating.

Due to the small size of the satellite and its spherical shape, we will consider it a one-node satellite. Then, by putting all the relevant values in equation (5.6), we find that in broad illumination the equilibrium temperature is 310 K, while during eclipse it descends to 240 K. In both cases, these values are close to the operational limits.

Several points make this calculation somewhat extreme. First, due to our supposition of one-node satellite it assumes that the equilibrium temperature is achieved in all the system (isothermal satellite), something that is not too close to reality for different reasons. The most important is the layer of aerogel, with its very low thermal conductivity that probably will damp the temperature excursions in the femtosatellite active parts.

Taken everything into account, it seems safe to claim that a passive thermal control is able to keep the satellite inside the operational temperature range (which has been shown to be [–40ºC,+85ºC] except for the flash memory; see chapter 4).

5.3 Battery endurance

We have determined the expected life of the femtosatellite in terms of the battery duration, which presents an electric charge (Q) of 9000 mAh or 32400 C as we can see in the equation (5.7). First of all, it has been calculated the total stored energy of the battery (E), which is equivalent to 32.4 Wh, by means of the equation (5.8). Then, it has been calculated the power of each electric component that constitutes the femtosatellite. The total power of the GPS is 0.043 W. Regarding the flash memory, it has been calculated both its nominal (0.039 W) and standby** power (0.0001 W). It is important to mention that the flash memory would work during the 10% of the total

time. The total power of the transmitter is 1.65 W and it would work the 0.37% of the total time (20 s per orbit of 90 min). Regarding the three accelerometers, we can see both the power of a single accelerometer (0.051 W) and the three together (0.153 W). The total power of the microcontroller working in RC_Run mode and with an oscillator frequency of 1 MHz is 0.002 W. Furthermore, it has been calculated the power of a single voltage regulator (0.013 W) and the two together (0.026 W). Finally, it has been determined the total battery life of the femtosatellite by means of the equation (5.9), which is around 6 days.

$$Q = 9000\,mA \cdot h = 9\,A \cdot h = 32400\,C \tag{5.7}$$

Then, the total energy stored in the battery is

$$E = V \cdot Q = 3.6\,V \cdot 32400\,C = 116640\,J = 32.4\,W \cdot h \tag{5.8}$$

Looking at table 4.1, we can make a list of the power consumptions by the different devices:

$P_{\text{GPS}} = 0.029\ \text{W}$
$P_{\text{fm-nominal}} = 0.039\ \text{W}$
$P_{\text{fm-standby}} = 0.0001\ \text{W}$
$P_{\text{transmitter}} = 1.65\ \text{W}$
$P_{\text{accelorometer}} = 0.051\ \text{W}$
$P_{\text{T-accelerometers}} = 0.153\ \text{W}$
$P_{\text{microcontroller}} = 0.002\ \text{W}$
$P_{\text{vr}} = 0.013\ \text{W}$
$P_{\text{T-vr}} = 0.026\ \text{W}$

Then, we can determine the time that the battery will endure before losing all its stored energy by means of the following equation (where it has been taken into account that not all systems are simultaneously active, especially the transmitter):

$$t \cdot (0.029\,W + 0.153\,W + 0.002\,W + 0.026\,W) + 0.1 \cdot t \cdot 0.039\,W + 0.9 \cdot t \cdot 0.0001\,W + 0.0037 \cdot t \cdot 1.65\,W = 32.4\,W \cdot h \tag{5.9}$$

with that we find that

$$t = 147.21\ \text{h} \approx 6\ \text{days}$$

This is marginally inferior to the requirement of one week for the lifetime of the femtosatellite (requirement 4 of section 3.3)

5.4 Expected orbital lifetime

It is quite obvious that a satellite subjected to aerodynamic drag will see a reduction of its orbital semimajor axis, and will eventually re-enter the atmosphere to be burned. Here we have performed just a rough approximation to the expected time to re-entry. To do so, we follow the treatment in SMAD [16].

Then, the drag results in orbital shrinking (and so on environment density, and orbital velocity increases), which can be given in terms of the relevant environmental and orbital parameters as

$$\Delta a = -2\pi \frac{C_D S}{m} \rho a^2 \qquad \textbf{(5.10)}$$

which can be used to show that the satellites would reside in orbit for only a few weeks (depending on the state of solar activity its ballistic coefficient $C_D S/m$).

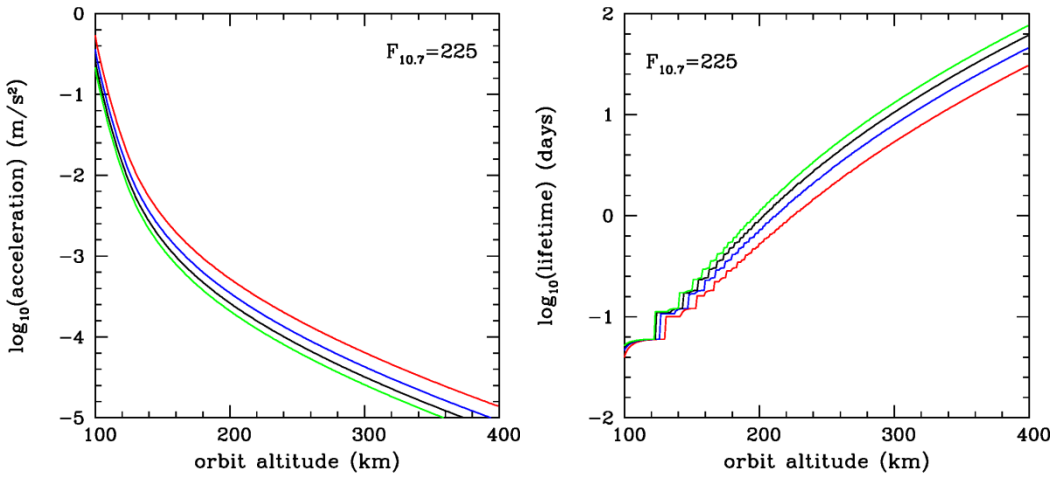

Figure 5.1 Deceleration of the femtosatellites (left) for ballistic coefficients of 20, 30, 40 and 50 kg/m^2. Orbit lifetimes for the same set of ballistic coefficients (right). All cases are for active Sun conditions ($F_{10.7}$ = 225).

It must be stressed that the ballistic coefficients shown are only representative values. Until the final decision has been made as to the total radius of the satellite, the ballistic coefficient will remain undetermined.

As is reasonable, the larger the ballistic coefficient, the longer the femtosatellite will in in orbit, but the lower the acceleration to be measured. So, a suitable, balanced choice must be made, taking also in consideration issues related to battery capacity and operational lifetimes.

Chapter 6

CONCLUSIONS AND FUTURE WORK

These are the main conclusions of this project:

- It has been achieved a preliminary design of the femtosatellite that would carry out the desired mission. This design complies with all the requirements posed by the scientific mission. Nevertheless, some improvement could be obtained for some of them.
- It has been done an exhaustive study of the current designs and tests of femtosatellites carried out by different institutions, and a research of the flight history of this category of satellites.
- The proper selection of all the electronic components that constitutes the satellite, such as the use of low power consumption COTS (Commercial-off-the-shelf) components, has allowed achieving a total battery life of around six days. A bit under our expectations.
- Three different analytic models or methods have been explained to determine the drag coefficient (C_D), and thus being able to determine the density in a certain point of the thermosphere. In the final design of the femtosatellite, we are going to use just one of this models.
- The inertia tensor of the femtosatellite has been calculated and modified by means of a 3D CAD software (SolidWorks ®) in order not to have a preferred rotation axis, in such a way that it would behave like a spherical spinning top. Hence, this would avoid the degradation of a specific part of the satellite surface by the atomic oxygen. In order to modify the inertia tensor, it has been placed six ballast spheres along the major axes of the femtosatellite. The total mass of the satellite is just under 100 grams, thus qualifying it as a femtosatellite.
- Speaking in general terms, we have achieved all the objectives of this work

It is obvious that the work is far from finished. There are several topics that have not been properly addressed, and that merit an in-depth study. First among those is the problem of launching the swarm. Sending the whole fleet of femtosatellites in a single cloud could be made with almost any launcher (one thousand femtosatellites having a mass of just 100 kg); but deploying them in several orbits with different inclinations is far from trivial. It seems that this orbital arrangement would demand several (simultaneous) launches, which would escalate the cost far beyond a reasonable cost. There is also the problem of volume, as the mass is quite reduced, but the volume is significant, especially for a secondary payload.

A very relevant, as well as quite difficult, subject is that of aerothermal heating. This term can be the limiting factor at low altitudes, becoming even comparable with solar energy flux, and thus forcing the temperature of the femtosatellites beyond the operational hot limit.

The mission overview and analysis demands a much thorough study. The one presented in this work is just a first order approach, needed to get a first order approximation for the requirements. So, a detailed orbital and performance analysis is required to further advance this proposal.

A reasonable next step is to build the system and test its performances. Here the problem would be associated with noise. Probably the tests would need to be performed in vacuum and at controlled temperature, but this is a problem that is beyond the scope of this Master Thesis.

REFERENCES

[1] Waldron et al., “The West Ford Payload”, Proceedings of the IEEE, may 1964, pp. 571–576.

[2] Orbital Debris Quarterly News, “West Ford Needles: Where Are They Now?”, vol 17, pp. 3–4 (2013)

[3] http://orbitaldebris.jsc.nasa.gov/measure/oderacs.html

[4] http://www.popsci.com/technology/article/2011-04/cornells-tiny-chip-sats-are-headed-iss-could-soon-be-bound-saturn

[5] Stuurman, B.; Kumar, K.D. RyeFemSat: Ryerson University: Femtosatellite Design and Testing; SpaceOps 2010 Conference **21**, pp. 25-30, doi: 10.2514/6.2010-2157. (2010)

[6] Barnhart, D.J., Vladimirova, T., Baker, A.M., & Sweeting, M.N., “A low-cost femtosatellite to enable distributed space missions,” *Acta Astronautica* **64**, pp. 1123-1143, doi:10.1016/j.actaastro.2009.01.025. (2009)

[7] Hedin, A. E., “Extension of the MSIS Thermosphere Model into the Middle and Lower Atmosphere”, *Journal of Geophysical Research: Space Sciences* **96**, 1159–1172 (1991)

[8] http://www.nrl.navy.mil/research/nrl-review/2003/atmospheric-science/picone/

[9] Bowman, B. R., Marcos, F. A., and Kendra, M. J., “A method to compute accurate daily atmospheric density values from satellite drag data”, AAS-04-173, *AAS/AIAA Flight Mechanics Meeting*, Maui (2004)

[10] Hedin, A.E., Spencer, N.W., and Killeen, T.L., “Empirical Global Model of Upper Thermosphere Winds Based on Atmosphere and Dynamics Explorer Satellite Data”, *Journal of Geophysical Research* **93**, 9959–9978 (1988).

[11] Hedin, A. E., et al., “Revised Global Model of Thermosphere Winds Using Satellite and Ground-Based Observations”, *Journal of Geophysical Research* **96**, 7657–7688 (1991).

[12] Hedin, A. E., et al., “Solar activity variations in the mid-latitude thermospheric meridional winds”, *Journal of Geophysical Research* **99**, 17601–17608 (1994)

[13] Hedin, A. E., et al., “Empirical wind model for the upper, middle and lower atmosphere”, *Journal of Atmospheric and Terrestrial Physics* **58**, 1421 –1447 (1996).

[14] http://www.atmop.eu/index.php/models

[15] http://energy.lbl.gov/ecs/aerogels/sa-physical.html

[16] Larson, W., & Wertz, J., *Space Mission Analysis and Design*, 3rd Edition, Kluwer (1999)

[17] www.genso.org

[18] Huang, A., Hansen, W.W., Janson, S.W., & Helvajian, H., "Development of a 100 g class inspector satellite using photostructurable glass ceramic materials," *Proceedings of SPIE- Photon Processing in microelectronics and photonics*, San Jose California, Vol. 4637, pp. 297-304. (2002)

[19] Janson, S., Huang, A., Hansen, W.W., & Helvajian, H., "Development of an Inspector Satellite Propulsion Module Using Photostructurable Glass/Ceramic Materials", CANEUS 2004 Conference on Micro-Nano-Technologies DOI: 10.2514/6.2004-6701

[20] Picone, J.M., Hedin, A.E., Drob, D.P. and Aikin, A. C., "NRL-MSISE-00 Empirical Model of the Atmosphere: Statistical Comparisons and Scientific Issues," *Journal of Geophysical Research*,

[21] ECSS, "Space Environment", ECSS-E-ST-10-04C, release November 15, 2008 (2008)